

## DISSOLVABLE METAL SUPPORTS FOR PRINTED METAL PARTS

Christopher S. Lefky<sup>1</sup>, Abdalla R. Nassar<sup>2</sup>, Timothy Simpson<sup>2,3</sup>, Owen J. Hildreth<sup>1\*</sup>

<sup>1</sup> School for Engineering Matter, Transport, and Energy, Arizona State University, Tempe, AZ 85287, USA

<sup>2</sup> Center for Innovative Materials Processing through Direct Digital Deposition, Pennsylvania State University, State College, PA, 16802, USA

<sup>3</sup> Mechanical Engineering & Industrial Engineering, Pennsylvania State University, University Park, PA 16802

\* Contact: Owen Hildreth, owen.hildreth@asu.edu

### Abstract

Temporary support structures are an inconvenient necessity in Direct Energy Deposition (DED) and Powder Bed Fusion (PBF) printed metal parts. Used to reduce thermal distortion and brace large overhangs, support structures often require post-print machining operations to remove, adding costs and processing delays. This preliminary work demonstrates that soluble, sacrificial metal supports can be fabricated in DED and PBF printers by taking advantage of small differences in the chemical and electrochemical stability between different metallic alloys. For DED printing, we demonstrate this process by printing stainless steel bridge structure with 90° overhang and printed carbon steel acting as a sacrificial support. For PBF printing, a PBF printed stainless steel part was first printed and then carburized to reduce the free chromium at the surface. Since the support/component interface is only ~100 μm in size, this interface becomes highly susceptible to chemical and electrochemical dissolution. In both cases, the component was separated from the supports in a solution of nitric acid and KCl under mild electrochemical bias. No machining, grinding, or finishing operations were required to remove the metallic supports. These novel approaches introduce new capabilities to additive manufacturing that will drastically reduce the post-processing needed for 3D printed metal components.

### Introduction

Additive Manufacturing (AM) of metal components can be classified by their binding method (sintering, melting, polymer adhesive), energy delivery method (laser, electron beam), and metal feed method (powder-bed, powder-fed, wire-fed). Metal components are commonly built using one of two methods: Powder-Bed Fusion (PBF) or Directed-Energy Deposition (DED).<sup>1</sup> In PBF, a laser or electron beam is scanned over a bed of metal powder to locally sinter or melt the powder, forming a slice of a part. Building up a sequence of slices by with more powder and sintering layers forms a complete 3D metal component.<sup>1</sup> In DED printing, metal powder(s) are blown or a wire is fed into a melt pool formed by a laser or electron beam. This added material increases the melt-pool and parts are built up in a layer-by-layer manner by moving the substrate relative to the energy/material deposition head.

Components printed using PBF and DED printers often require support structures to minimize thermal distortion and form overhanging structures.<sup>2,3</sup> Unfortunately, removing these support structures can require extensive post-process machining; which can add enough cost and processing time to outweigh any benefits associated with additive manufacturing. The plastics extrusion 3D printing community has already solved this problem by printing parts and supports out of polymers with different solubilities. For example, components are printed using Acrylonitrile Butadiene Styrene (ABS) and sacrificial supports printed using Polylic Acid

(PLA). After printing, the PLA is selectively dissolved by immersing the printed structure in a solution of isopropyl alcohol and potassium hydroxide with the ABS component left intact.<sup>4</sup>

This manuscript summarizes new advances in dissolvable metal supports for AM manufactured metal components. Using DED printing, we recently demonstrated that the concept of selectively soluble support dissolution can be applied to 3D printed metal structures.<sup>5</sup> Specifically, we demonstrate that AISI type 431 (Fe 16Cr 2Ni 0.2C) stainless steel parts with free standing bridge structures with overhangs of 90° can be fabricated using Metco 91 (mild steel) carbon steel as the sacrificial support structure. This support structure was removed using a solution of nitric acid with an applied external electrochemical bias to increase removal rate. While this set of experiments validated the concept of soluble metal supports, only a small fraction of the 3D metals printing community has access to multi-material DED printers. Instead, the community largely uses PBF printers that only print one material at a time. In this manuscript, also demonstrate a new process that brings dissolvable supports to single-material printed components. In this new process, we degrade the chemical resistance of the top ~100 μm of the printed structure using simple surface treatments incorporated into the thermal stress relieving step. Since support support/component interface is only 100-200 μm in diameter, the component is readily separated from the supports using chemical or electrochemical methods.

This work draws heavily from the concept of sacrificial anodes. A sacrificial anode is a material with a more negative redox potential relative to the part material such that the sacrificial anode will be preferentially oxidized over the part material.<sup>6</sup> For example, a zinc anode (standard reduction potential,  $E_o^{Zn} = -0.76 \text{ V}$ )<sup>7</sup> is often used to protect stainless steel boat hulls since the standard reduction potential of Zn is lower than both the base iron ( $E_o^{Fe} = -0.44 \text{ V}$ )<sup>7</sup> and the passivating chromium oxide layer ( $E_o^{Cr_2O_3} = 1.3 \text{ V}$ )<sup>7</sup> that forms in stainless steel. As long as the zinc is in electrical and electrolytic contact with the stainless steel hull, then the zinc will preferentially oxidized to  $Zn_{aq}^{2+}$  instead of the steel. For metallic alloys, the corrosion potential depends not just on redox potential of the constituent elements, but also microstructure, passivation, and electrolyte composition.<sup>8-15</sup> As a result, small changes in composition or microstructure can result in very large differences in corrosion resistance. This manuscript presents two different methods to generate composition and microstructure differences between the support and component part such that the support structures are preferentially etched. The first method used a multi-material DED printer to print dissolvable carbon steel supports for a stainless steel component. The second method used a single-material PBF printer to print a stainless steel part that is next sensitized using carburization/nitridation to captures the chromium in carbides/nitrides and lowers the corrosion resistance of the stainless steel to a depth of ~100 μm. Since the support structures only contact the part across 100 μm, the supports are easily dissolved away from the component.

For DED, the proof-of-concept system comprised of stainless steel as a component material, carbon steel as a sacrificial anode support material, and 41 wt.% nitric acid as the corrosive electrolyte. Stainless steel has excellent resistance to nitric acid while carbon steel is rapidly chemically dissolved nitric acid with or without an external bias.<sup>8,16,17</sup> A free standing stainless steel bridge was fabricated using a DED powder-fed process by printing a stainless steel bridge with a carbon steel support across the middle and then etching away the carbon steel in nitric acid with bias of 700 mV to 900 mV relative to a the Saturated Hydrogen Electrode.

Since multi-material PBF printers are not yet widely available, a surface-treatment approach for dissolvable supports was developed for use in single-material systems. For a demonstration, a component part with attached supports was printed from PH 17-4 stainless steel. After printing, the part was packed with sodium ferrocyanide hydrate and was heated to 800 °C for six hours. This treatment both reduced internal thermal stresses and diffused carbon and nitrogen into the top 100 μm to 200 μm of the PH 17-4. At this temperature, the carbon and nitrogen capture much of the available chromium in chromium carbides and nitrides. Once the free chromium content drops below 10.5 wt.%, the material is no longer “stainless” and readily dissolves under bias in nitric acid solutions. The supports were separated from the component at -150 mV<sub>SHE</sub> bias in a solution of 3 wt.% nitric acid and 0.1 molar KCl.

This work is the first to demonstrate dissolvable support strategies for both multi-material printing systems (*e.g.*, DED) and single-material printing systems (*e.g.*, PBF). These sacrificial materials will eliminate or reduce the need for post-process machining operations in 3D printed metals. Since both processes are “self-

terminating,” they are extremely easy to implement and should free the design of AM fabricated metal components from the constraints of providing access to machining tools.

## **Experimental Methods**

### **DED Sample Fabrication**

DED samples were fabricated using an Optomec Laser Engineered Net Shaping (LENS) MR-7, directed energy deposition system with two powder feeders was used for metal deposition. The system was equipped with a 500-watt Ytterbium-doped fiber laser (IPG YLR-500-SM). A second-moment beam spot size of 1.2 mm was measured, using a PRIMES GmbH FocusMonitor, at the substrate location. Before deposition, the substrate was positioned at a working distance of 9.3 mm from four, radially symmetric powder-delivery nozzles. AISI type 431 (Fe 16Cr 2Ni 0.2C) and Metco 91 (mild steel) structures were deposited atop 304 Machinable Stainless Steel substrates. Prior to support dissolution, substrates were mounted in nitric acid resistance epoxy (Epoxy Systems, Inc., 633 Grey), cleaned with acetone and isopropyl alcohol and dried using N<sub>2</sub> gas. See previous work for more detailed fabrication specifications.<sup>5</sup>

All chemicals were used as received. The electrolyte solution was made by mixing 70 wt.% nitric acid (Sigma Aldrich, ACS reagent, 70 wt.%) with deionized water (18.2 MΩ, Purelab Flex 3) at a volume ratio of 1:1 – HNO<sub>3</sub>:H<sub>2</sub>O to form a final volume of 200 mL and a 41 wt.% nitric acid solution. Next, 8 grams of KCl was added to improve the electrical conductivity of the electrolyte and help break down the passivation that forms on carbon steel parts in nitric acid.<sup>8</sup>

### **PBF Sample Fabrication and Sensitization**

PH 17-4 samples were produced using an EOS M280 PBF system and built using the OEM’s standard parameters and powder for PH 17-4 (EOS StainlessSteel GP1) with a 20 μm layer height. Sample specimens were cut from a tubular arch with a measured OD of 8.16 mm, ID of 3.13 mm, and a major radius of 46 mm. The samples were sonicated in acetone, then isopropyl alcohol, and finally dried using N<sub>2</sub> gas. Next, samples were dipped in a saturated solution of sodium ferrocyanide decahydrate (Na<sub>4</sub>Fe(CN)<sub>6</sub> · 10H<sub>2</sub>O, Sigma Aldrich, ≥99%) allowed to air-dry, and placed on stainless steel tool wrap. A sodium ferrocyanide paste (5.4 grams Na<sub>4</sub>Fe(CN)<sub>6</sub> · 10H<sub>2</sub>O, 1.3 mL DI H<sub>2</sub>O) was packed around the part and the tool wrap was folded and sealed around the part. A small hole was punctured into the stainless steel wrap to outgas the ~0.25 moles of CN and H<sub>2</sub>O vapor that could be produced as the sodium ferrocyanide decahydrate decomposes. Samples were then placed into an exhausted box furnace at 800 °C for six hours and allowed to cool to room temperature overnight in the oven. Samples were removed from the foil and excess decomposition products were removed using stainless steel bristle brush followed by sonication in DI H<sub>2</sub>O and isopropyl alcohol.

### **Electrochemical Analysis and Dissolution**

#### *DED Support Removal*

All chemicals were used as received. The electrolyte solution was made by mixing 70 wt.% nitric acid (Sigma Aldrich, ACS reagent, 70 wt.%) with deionized water (18.2 MΩ, Purelab Flex 3) at a volume ratio of 1:1 – HNO<sub>3</sub>:H<sub>2</sub>O to form a final volume of 200 mL and a 41 wt.% nitric acid solution. Next, 8 grams of KCl was added to improve the electrical conductivity of the electrolyte and help break down the passivation that forms on carbon steel parts in nitric acid.<sup>8</sup> Immediately prior to electrochemical analysis/dissolution, the samples were sonicated in acetone, then isopropyl alcohol, and finally dried using N<sub>2</sub> gas.

A Pine Research Instruments WaveNow USB Potentiostat/Galvanostat was used to measure the Open-Circuit Potential (OPC), gather potentiodynamic polarization curves, and apply constant bias for electrochemical dissolution of the mixed stainless steel/carbon steel part. All measurements were made relative to a saturated silver/silver chloride electrode in a saturated KCl solution. The reference electrode was interfaced to the etching electrolyte through a glass-fritted salt bridge with 4 M KCl (Alfa Aesar, 99%) intermediate electrolyte; the glass frit was located approximately 1.0 mm from the working electrode (*i.e.* 3D printed sample). The measured Potentials, *E*, were offset by +0.197 mV so that all reported values are relative to the

Standard Hydrogen Electrode (SHE). A 6 mm diameter graphite rod was used as the counter electrode. The electrodes were positioned in a line with the reference electrode between the working and counter electrodes.

### *PBF Support Removal*

An electrolyte of 3 wt.% nitric acid with 0.1 molar KCl was made by mixing 70 wt.% nitric acid with DI H<sub>2</sub>O, and KCl. Using the same setup as the DED support removal process, OPC and potentiodynamic curves were gathered from the untreated part, treated part, and post-etched component to identify the corrosion potential and potential to selectively etch the sensitized surface without etching the component. The sample was etched between 99-444 mV<sub>SHE</sub> for 12.75 hours until the component separated from the part. The sample was removed every sixty minutes for optical imaging. After eight hours, the build-up of black powder (presumably magnetite, Fe<sub>3</sub>O<sub>4</sub>) within the supports was removed using a steel wire brush and the sample was etched for two more hours until the component separated from the supports.

## **Results and Discussion**

### **Dissolvable DED Supports**

The full details of the dissolvable DED support structures can be found in the author's previous work.<sup>5</sup> The corrosion potential,  $E_{corr}$ , of the AISI type 431 stainless steel, Meco 91 carbon steel, and the mixed printed part were measured at 1.113 V<sub>SHE</sub>, 1.004 V<sub>SHE</sub>, 0.197 V<sub>SHE</sub> respectively. As expected, the stainless steel shows a more positive  $E_{corr}$  than both the mixed sample and the carbon steel sample. More importantly, polarization curves showed that carbon steel etches many orders of magnitude faster than the carbon steel across wide range of potentials.<sup>5</sup>

Electrochemical etching the mixed stainless/carbon steel sample was conducted by setting a constant potential (typically between ~800 mV<sub>SHE</sub> to 900 mV<sub>SHE</sub>) to create a slight anodic current, typically on the order of -10 mA to -50 mA, with no O<sub>2</sub> bubbling but >100 mA with O<sub>2</sub> bubbling. Since the Pinewave Now potentiostat is limited to ±105 mA and was often driven to maximum current, the actual applied varied with the formation of passivating layers, changing surface area, and bubble entrapment within the stainless steel bridge. Under potentials between ~700 mV<sub>SHE</sub> to 900 mV<sub>SHE</sub>, a cyclic shift from anodic to cathodic with a periodicity between 50 to 500 seconds was observed as a passivation layer on the carbon steel forms and dissolves.<sup>5</sup> Under potentials between ~700 mV<sub>SHE</sub> to 900 mV<sub>SHE</sub>, a cyclic shift from anodic to cathodic with a periodicity between 50 to 500 seconds was observed as a passivation layer on the carbon steel forms and dissolves.<sup>5,18</sup> Under these conditions, the stainless steel is well protected; however, the etch rate is too slow for practical applications, and it took ten hours to remove 1.4 mm of carbon steel from each end. The etch rate was increased significantly by bubbling O<sub>2</sub> onto the carbon steel section of the part. The O<sub>2</sub> helps break down passivated carbon steel, and a cathodic current was observed. This increases the etch rate dramatically, and the remaining 7 mm of the carbon steel section was removed in 6 hours. This constant cathodic current was not observed when bubbling O<sub>2</sub> onto the stainless steel section of the sample. Figure 1 shows the sample before and after etching. Notice that the carbon support material was completely removed during the etching process. The support removal process is, effectively, self-terminating and should be robust for manufacturing applications.

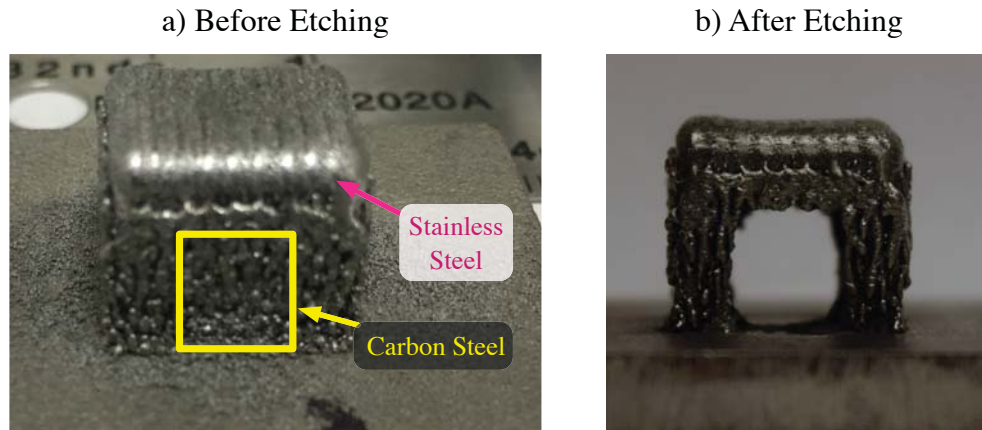


Figure 1. Digital images of the sample taken before and after etching. (a) Before etch, red square roughly outlines where the carbon steel support layer was printed. (b) After etching showing that the carbon steel was completely etched from the sample.<sup>5</sup>

### Dissolvable PBF Support Structures

As a demonstration, a simple tubular arch was printed from PH 17-4 stainless steel using PBF printer. Sections of the part were cut from the tube (see Figure 2a) and subject to a sensitization processes to capture the free-chromium within the top  $100\ \mu\text{m}$  –  $200\ \mu\text{m}$  of the surface. While there are numerous ways to capture this chromium, this concept was demonstrated with a standard “packed” carburization process that used sodium ferrocyanide as the carbon and nitrogen source. The sample was packed with sodium ferrocyanide and treated for six hours at  $800\ ^\circ\text{C}$ . At this temperature, chromium carbide precipitates readily form at the grain boundaries<sup>19</sup> and the available “free-carbide” drops below the 10.5 wt.% necessary to sufficiently passivate the part with protective chromium oxide where the carbon content was high enough.

The sample was examined and etched in a 3 wt.% nitric acid solution with 0.1 molar KCl added to improve the conductivity of the solution. The measured OPC of the untreated, sensitization treated, and post-etch component were  $365\ \text{mV}_{\text{SHE}}$ ,  $-22\ \text{mV}_{\text{SHE}}$ ,  $363\ \text{mV}_{\text{SHE}}$  respectively. To dissolve off the supports, an anodic potential between  $99\ \text{mV}_{\text{SHE}}$  to  $444\ \text{mV}_{\text{SHE}}$  was applied for 8 hours with the sample removed every hour for optical imaging. During this time, the corrosion current was observed to decrease over time even with anodic potentials were applied. A buildup of black powder was observed over the sample and was suspected of restricting electrolyte access to the sample surface. A steel wire brush was gently applied to the sample surface followed by sonication, a dark black powder was observed coming off the sample. This process was repeated eight times until no more powder was observed. After this first cleaning process, the measured current returned to 80 mA. This verified that precipitate build-up was responsible for the drop in current, future work will add HCl to dissolve the precipitated manganite and avoid this build up. For this work, the precipitate was removed using wire-brushing and sonication; although less extensive cleaning was needed for the remainder of the etching process. The sample was etched for another 3.5 hours before the component separated from the supports.

The optical images in Figure 2a-f shows the sample as it when through this new process. Figure 2a shows the original printed sample. The “component” is the round tubular section on the left. Notice that the supports connect to the component at fine points less than  $100\ \mu\text{m}$  in size. After heat treatment, Figure 2b, the sample is darkened in color and some of the voids between the sample and the component have been filled in with excess carbon. Although not applied in this experiment, this excess carbon can be easily burned away to increase the initial etch rate. Figure 2c shows the sample after eight hours of etching with no brushing. Notice that the component still appears dark in color, indicating that the carburized layer has not been fully removed. Additionally, only a small percentage of the supports have been removed by this time. Brushing and sonicating the sample to remove precipitate buildup increases the etch rate significantly. Figure 2d-f show significant support dissolution over the 3 hours with component separating with no mechanical machining operations.

Notice that by Figure 2d, the component appears bright black. This indicates that the etching has reached the underlying stainless steel. The diameter was measured after sensitization and hourly after eight hours. The original diameter was 8.16 mm after eight hours of etching the diameter decreased to 7.85 mm. By nine hours (after brushing) of etching the underlying stainless steel was revealed and the diameter was measured at 7.78 mm and did not decrease or change with further exposure to the etching environment; indicating that the process is self limiting and can be conducted without overly-detailed monitoring. Future work will eliminate the need for the brushing and sonication steps by adjusting the electrolyte to dissolve and reaction products.



Figure 2. Camera images of sample. a) as printed; b) after sensitization treatment; c) after 8 hours of etching. Notice that the surface of the component (round section) is still black in color and that the etch rate appears slow when magnetite isn't removed from the surface. d) after 9 hours (total) of etching with wire-brushing. Notice that the component is now shiny and bright; indicating that the stainless steel layer has been reached. e) after 10 hours (total) of etching. Notice that the component appears unchanged while most of the support structures have been dissolved; f) after 11 hours of etching. The component completely separated from the supports with no mechanical machining. Component appears largely unchanged.

## Conclusions

In conclusion, a method to form large overhangs and dissolvable support structures in parts fabricated using DED and PBF additive manufacturing. For DED, a stainless steel bridge was fabricated using carbon steel that was later removed by electrochemically etching the carbon steel in a 41 wt.% solution of nitric acid with bubbling  $O_2$ . For PBF, a stainless steel sample was fabricated and then sensitized using a carburization process

that effectively converted the top  $\sim 100\ \mu\text{m}$  of stainless steel to carbon steel. This layer was electrochemically etched in a 3 wt.% nitric acid solution with 0.1 molar KCl. The supports were easily separated with no mechanical machining operations. This first-of-its-kind approach introduces new capabilities to additive manufacturing and may drastically reduce the post-processing needed for metal parts thereby reducing process costs while simultaneously increasing design freedom. Additionally, we expect this process to be applicable to a wide range of metals and even oxides through selective chemical dissolution.

### Acknowledgements

Hildreth gratefully acknowledges funding for this project provided by Science Foundation Arizona for (BSP 0615-15).

### References

- (1) Gibson, I.; Rosen, D. W.; Stucker, B. *Additive Manufacturing Technologies*; 1st ed.; Springer US: New York, NY, 2010.
- (2) Di Wang; Yang, Y.; Yi, Z.; Su, X. Research on the Fabricating Quality Optimization of the Overhanging Surface in SLM Process. *Int J Adv Manuf Technol* **2013**, *65*, 1471–1484.
- (3) Griffith, M. L.; Harwell, L. D.; Romero, J. T.; Atwood, C. L. Multi-Material Processing by LENS. *Solid Freeform Fabrication Proceedings* **1997**, 387–394.
- (4) Domonoky; BonsiBrain. Support - Full Disclosure <http://ifeelbeta.de/index.php/support/support-full-disclosure> (accessed Feb 2, 2016).
- (5) Hildreth, O.; Nassar, A. R.; Chasse, K. R.; Simpson, T. W. Dissolvable Metal Supports for 3D Direct Metal Printing. **2016**, *3*, 90–97.
- (6) Warren, N. *Metal Corrosion in Boats*; 3rd ed.; Sheridan House, Inc.: Dobbs Ferry, NY, 2006.
- (7) Haynes, W. M. *CRC Handbook of Chemistry and Physics, 95th Edition*; Haynes, W. M., Ed.; 96 ed.; CRC Press, 2014.
- (8) Epstein, J. A.; Levin, I.; Rabinovitz, E.; Raviv, S. Cathodic Corrosion of Stainless Steel in Nitric Acid. *Corrosion Science* **1965**, *5*, 461–470.
- (9) Sastry, T. P.; Rao, V. V. Anodic Protection of Mild Steel in Nitric Acid. *Corrosion* **1983**, *39*, 55–60.
- (10) Deakin, J.; Dong, Z.; Lynch, B.; Newman, R. C. De-Alloying of Type 316 Stainless Steel in Hot, Concentrated Sodium Hydroxide Solution. *Corrosion Science* **2004**, *46*, 2117–2133.
- (11) Laleh, M.; Kargar, F. Suppression of Chromium Depletion and Sensitization in Austenitic Stainless Steel by Surface Mechanical Attrition Treatment. *Mater Lett* **2011**, *65*, 1935–1937.
- (12) Johannes, A. C.; Farmer, J. C.; Brewer, L. N.; Osswald, S. Letting Corrosion Work for You: Novel Pathways to Additive Manufacturing and Nanomaterial Synthesis Using Electrochemically-Driven Powder Consolidation. *Advanced Engineering Materials* **2014**, *16*, 1147–1159.
- (13) Kim, H.-J.; Jeon, S.-H.; Kim, S.-T.; Lee, I.-S.; Park, Y.-S.; Kim, K.-T.; Kim, Y.-S. Investigation of the Sensitization and Intergranular Corrosion of Tube-to-Tubesheet Welds of Hyper Duplex Stainless Steel Using an Electrochemical Reactivation Method. *Corrosion Science* **2014**, *87*, 60–70.
- (14) Seikh, A.; Mohammad, A.; Sherif, E.-S.; Al-Ahmari, A. Corrosion Behavior in 3.5% NaCl Solutions of  $\Gamma$ -TiAl Processed by Electron Beam Melting Process. *Metals* **2015**, *Vol. 5*, Pages 2289-2302 **2015**, *5*, 2289–2302.
- (15) Dai, N.; Zhang, L.-C.; Zhang, J.; Chen, Q.; Wu, M. Corrosion Behavior of Selective Laser Melted Ti-6Al-4V Alloy in NaCl Solution. *Corrosion Science* **2016**, *102*, 484–489.
- (16) Kolman, D. G.; Ford, D. K.; Butt, D. P.; Nelson, T. O. Corrosion of 304 Stainless Steel Exposed to Nitric Acid-Chloride Environments. *Corrosion Science* **1997**, *39*, 2067–2093.
- (17) Ningshen, S.; Kamachi Mudali, U.; Ramya, S.; Raj, B. Corrosion Behaviour of AISI Type 304L Stainless Steel in Nitric Acid Media Containing Oxidizing Species. *Corrosion Science* **2011**, *53*, 64–70.
- (18) Evans, U. R. Behaviour of Metals in Nitric Acid. *T Faraday Soc* **1944**, *40*, 120–130.
- (19) Turpin, T.; Dulcy, J.; Gantois, M. Carbon Diffusion and Phase Transformations During Gas Carburizing of High-Alloyed Stainless Steels: Experimental Study and Theoretical Modeling. *Metall and Mat Trans A* **2005**, *36*, 2751–2760.